Title: Economic optimization of photovoltaic water pumping systems for irrigation

Authors: P.E. Campana[1], H.Li[1], J. Zhang[2], R. Zhang[3], J. Liu[2], J. Yan[1, 4]

[1]School of Business, Society & Engineering, Mälardalen University, SE-72123 Västerås, Sweden

[2]Institute of water resources and hydropower research, 100038 Beijing, China

[3]Institute of water resources for pastoral areas, 010020, Hohhot, China

[4]School of Chemical Science, KTH Royal Institute of Technology, SE-10044 Stockholm, Sweden

Corresponding author: P.E. Campana

Corresponding author's contact information: (Email) pietro.campana@mdh.se ; (Phone) +46 (0)21 101469

Economic optimization of photovoltaic water pumping systems for irrigation

P.E. Campana[1], H.Li[1], J. Yan[1, 2], J. Zhang[3], R. Zhang[4], J. Liu[3]

[1]School of Business, Society & Engineering, Mälardalen University, SE-72123 Västerås, Sweden

[2]School of Chemical Science, KTH Royal Institute of Technology, SE-10044 Stockholm, Sweden

[3]Institute of water resources and hydropower research, 100038 Beijing, China

[4]Institute of water resources for pastoral areas, 010020, Hohhot, China

Abstract

Photovoltaic water pumping technology is considered as a sustainable and economical solution to provide water for irrigation, which can halt grassland degradation and promote farmland conservation in China. The appropriate design and operation significantly depend on the available solar irradiation, crop water demand, water resources and the corresponding benefit from the crop sale. In this work, a novel optimization procedure is proposed, which takes into consideration not only the availability of groundwater resources and the effect of water supply on crop yield, but also the investment cost of photovoltaic water pumping system and the revenue from crop sale. A simulation model, which combines the dynamics of photovoltaic water pumping system, groundwater level, water supply, crop water demand and crop yield was validated against the measured data, is employed during the optimization.

To prove the effectiveness of the new optimization approach, it has been applied to an existing photovoltaic water pumping system. Results show that the optimal configuration can guarantee continuous operations and lead to a substantial reduction of photovoltaic array size and consequently of the investment capital cost and the payback period. Sensitivity studies have been conducted to investigate the impacts of the prices of photovoltaic modules and forage on the optimization. Results show that the water resource is a determinant factor.

Keywords: Photovoltaic water pumping system, irrigation, grassland desertification, field validation, optimization.

1 Introduction

Desertification, defined as land degradation resulting from both climatic-natural variations and human activities, is one of the most crucial worldwide environmental problems affecting food security, water security, eco-security, socioeconomic stability and sustainable development [1]. Photovoltaic water pumping (PVWP) systems, which can provide water for irrigation, have been considered a sustainable and economical solution to curb the progress of desertification [2].

There have been many studies regarding PVWP systems. For example, Bouzidi et al. [3] analysed the performances of such a system installed in an isolated site in the south of Algeria estimating the amount of water that could be supplied under different solar radiation conditions; similarly, Hrayshat and Al-Soud [4] studied the potential application of PVWP systems in Jordan; Bouzidi [5] compared PVWP systems with wind power water pumping (WPWP) systems to cover drinking water requirements in a specific location in Algeria; Ghoneim [6] developed a program for modelling each PVWP component to assess the

65 performance of PVWP systems in Kuwait; Benghanem et al. [7] studied the effect of pumping
66 head on the performance of PVWP systems using an optimal PV array configuration to drive a
67 direct current (DC) helical pump; Mokeddem et al. [8] investigated the performance of a
68 directly coupled PVWP system; Boutelhig et al. [9] compared two different DC pumps with the
69 scope of selecting the optimal direct coupling configuration for providing water to a farm in
70 Algeria; Hamidat at al. [10] presented the electrical and hydraulic performance of a surface
71 centrifugal pump as a function of the hydraulic head and size of PV array for irrigation
72 purposes in the Sahara region; Senol [11] focused on small and medium-size mobile PVWP
73 applications for watering purposes in Turkey; Glasnovic and Margeta [12] elaborated an
74 optimization model for small PVWP system for irrigation; Pande et al. [13] concluded that in
75 order to achieve a successful design of PVWP system, the water supply and crop water
76 requirements for orchards have to be carefully considered. Due to the extreme dynamic
77 variability of the parameters affecting the functioning of PVWP systems, principally solar
78 radiation, dynamic modelling is an important tool to evaluate their performances [14].
79 Campana et al. [15] modelled both the PVWP system and the crop water requirements to
80 analyse the match between water demand and water supply. Model validation for both PVWP
81 system and crop water requirement was presented in several works: Amer and Younes [16]
82 validated long term performance of PVWP system using a simple algorithm; Hamidat and
83 Benyoucef [17] validated PVWP system models based on the pump experimentation; Luo and
84 Sophocleous [18] validated the models for assessing crop water requirements using a
85 lysimeter. The technical advantages of a novel control system for achieving an optimal
86 matching between crop water demand and water supply and for interfacing PVWP systems to
87 the grid were analysed by Campana et al. [19]. The positive economic and environmental

88 aspects of the proposed novel control system for PVWP applications was studied by Campana
89 et al. [20].

90 Our effort focuses on the application of PVWP technology for irrigation to combat the
91 grassland degradation and to promote the farmland conservation in rural areas of China.
92 Previously, the estimation of the water demand for irrigation and the assessment of the
93 groundwater resources were carried out by Xu et al. [21]. Yu et al. [22] assessed the most
94 suitable areas for PVWP irrigation system in Qinghai Province and in the entire China. The
95 groundwater resource has been identified as a crucial factor concerning the implementation
96 of PVWP for irrigation [23]. The potential benefit of applying PVWP in the improvement of
97 biodiversity of grassland [24], carbon sequestration [25], and energy and food security [26]
98 were also investigated. A novel business model, which can be applied to integrated PVWP
99 systems for grassland and farmland conservation, was proposed, including environmental co-
100 benefits, agricultural products and social visualization of all benefits [27].

101 The PVWP technology is a well-developed technology with thousands of installations
102 worldwide. The common approach for optimizing a PVWP system mainly deals with the
103 improvement of effectiveness of various system components with the aim of minimizing the
104 total cost. However, Glasnovic and Margeta [12] pointed out that this approach suffers from
105 the lack of systematic quality and static quality. As a result it doesn't yield optimal results.
106 Therefore, a new optimization method, which integrated all relevant system elements and
107 their characteristics systematically, was developed. The objective function was still to
108 minimize the PV size; whereas, the constraints were defined in a new way, which considered
109 not only the water demand, but also the available water resource. The approach was tested
110 at two areas in Croatia. Smaller PV sizes and thus lower PV costs were achieved. Nevertheless,

111 the economic feasibility of PVWP is not solely determined by the investment cost of PVWP, it
112 is also tightly related to the benefit from the crop. Even though the investment cost is linearly
113 proportional to the PVWP size, the relationship between PVWP system size, crop yield and
114 pumped water is nonlinear. Hence, it is essential to include that benefit in the optimization of
115 PVWP systems. To the best knowledge of authors, there hasn't been any work regarding
116 optimizing PVWP with the consideration of crop benefit.

117 The main objective of this paper is thus to develop a new optimization method taking into
118 account the crop yield response to the supplied water and the revenue from selling the crop.
119 As the price of PV modules follows a trend of decrease while the price of crops follows a
120 country trend of increase, the sensitivity study will also be conducted in order to assess the
121 influences of those prices on the optimization. Different from the work carried out by
122 Glasnovic and Margeta [12] that statistic models were used for the simulation of PV system,
123 pumped water and water demand, the following hourly dynamic models are employed in this
124 paper: PV system, inverter-pumping system, water requirements, groundwater level and crop
125 yield response to water. In addition, the hourly models of PVWP system, crop water demand
126 and ground water level are validated against measurements, giving more accurate results. This
127 paper is organized as follows: section 2 presents the proposed optimization approach; section
128 3 introduces all the models adopted to describe the operation of a PVWP system and provides
129 the model validation; section 4 shows the results of optimization; and section 5 summarizes
130 the important findings of this work.

2 Optimization approach and models description

Genetic algorithm *GA* has been used to find the optimal PVWP system size, as well recognized optimization technique [28]. The optimization problem finds the optimal size of PVWP systems for irrigation using one objective function under a prerequisite. The objective function is to maximize the annual profit, given by the balance between annual revenue R_{ann} ($), annualized initial capital cost ICC_{ann} ($) and annual operation, maintenance and replacement cost omr_{ann} ($). It thus (I) maximizes the crop yield Y_a (tonne DM/ ha year) and consequently the annual revenue R_{ann} and (II) minimizes the PVWP system size and consequently the sum of annualized initial capital cost ICC_{ann} and the corresponding annual operation, maintenance and replacement cost omr_{ann}. The prerequisite is to have zero system failure or ensures the 100% reliability and sustainability of the PVWP system during the whole irrigation season. The PVWP system failure *f* is defined as the hourly drawdown s_h (m) (induced by the pumping system during the irrigation season) goes below the level of pump h_p (m) (measured from the static water level) or the daily water pumped volume $V_{p,d}$ (m^3) is larger than the daily sustainable pumped water volume $V_{s,d}$ (m^3). Different from previous optimization works, the following constraints are carefully considered in this work: the hourly decline of the groundwater level *s* and the daily pumped water limited by the water resource $V_{p,d}$. *s* and $V_{p,d}$ dynamically depend on the PVWP system capacity and water resource. If those two constraints are not taken into account in the optimization process, the PVWP system capacity can be oversized resulting in the dry-up of well, the broke-down of the pump, and the failure of sustainable water management. Furthermore, an oversized PVWP system also implies higher initial capital costs. The mathematical formulation of the proposed optimization approach is given by the following set of equations:

$$max(R_{ann} - ICC_{ann} - omr_{ann}) \quad (1)$$

$$\sum f = 0 \ \left(f = \{0,1\}, f = 1 \ if \ s_h > h_p \ and \ V_{p,d} > V_{s,d}\right) \quad (2)$$

The annual revenues R_{ann} from the forage sale depends on the actual forage yield Y_a and the specific forage price p_f ($/tonne DM) according to the following equation:

$$R_{ann} = Y_a p_f \quad (3)$$

The actual forage yield Y_a is a function of the pumped water and thus PVWP system capacity and it has been dynamically calculated according to the procedure described in section 3.4. The specific forage price p_f has been assumed equal to 207 $/tonne DM [29]. The ICC_{ann} has been calculated from the initial capital cost *ICC* with the following equation:

$$ICC_{ann} = ICC \left[\frac{i(1+i)^n}{(1+i)^n - 1}\right] \quad (4)$$

Where, *i* and *n* are the real interest rate and the project lifetime assumed equal to 6.4% [30] and 25 years, respectively. The *ICC* of PVWP systems has been estimated from the capacity according to the data provided by a manufacturer company [31]. The PVWP system and components costs are depicted in Figure 1 as a function of the capacity. The PV modules price has been assumed equal to 1, 1.5 and 2$/$W_p$ to conduct a sensitivity analysis. The specific inverter and pump costs have been assumed equal to 0.5 and 0.15 $/W, respectively [31]. The project implementation costs have been set equal to 30 % of the PVWP components cost, including cost for design and installation [31].

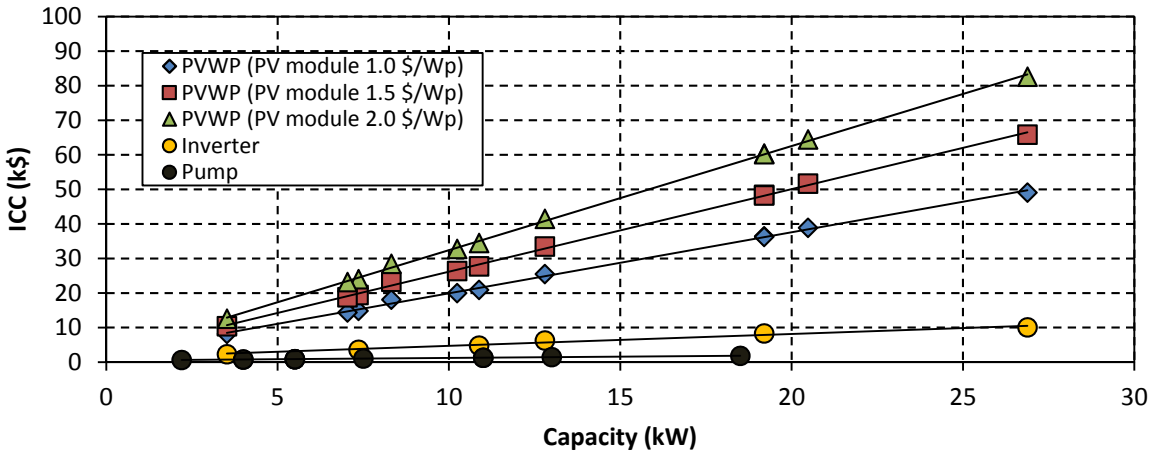

172

173 Figure 1: PVWP system initial capital cost as a function of the capacity [31].

174 The annual operation, maintenance and replacement cost omr_{ann} has been set to 4% of the
175 *ICC*, assuming an annual operation and maintenance cost equal to 2% of the *ICC* and assuming
176 to replace the pump and the inverter every 8 years. The assessment of the PVWP system
177 profitability has been carried out using the payback period *PBP* as in previous economic
178 analysis conducted for PVWP systems for irrigation [32]. The optimization is conducted using
179 Solve XL, an add-in for Microsoft Excel that gives the possibility to use *GA* to solve various
180 optimization problems [33]. The optimization parameters for setting the *GA* are shown in
181 Table 1.

182 Table 1: Genetic algorithm parameters [33].

Population size	200
Algorithm	NSGA 2
Crossover rate	50%
Selector	Crowded tournament
Mutation rate	5%

Number of generations	200

To optimize the PVWP system, the decision variables include: (I) the PV power peak capacity that has direct effects on the PVWP initial capital costs, volume of pumped water and crop yield and thus annual revenues. It varies in the range of 0 to 3.2 kW_p; (II) the tilt angle β (˚) and (III) the azimuth angle γ (˚) that have direct effects on the harvested solar irradiation and thus indirectly on the PVWP system size. β and γ vary in the range of 0˚ to 50˚ and -30˚ to 30˚, respectively. The pumping system capacity has not been considered as decision variable but chosen on the basis of the PVWP system size. Three different pumps capacities and their relative operating curves have been considered: 1.1 kW, 1.5 kW and 3.2 kW, respectively. If the optimal PV size exceeds the pump capacity 30%, then the upper pump capacity is selected. The optimization problem finds the optimal solution in terms of tilt angle, azimuth angle and PV power peak capacity that allows to increase the profit without violating the groundwater level constraint.

It has to be emphasized that the optimization conducted by Glasnovic and Margeta [12] was based on decade time step, which cannot reflect the intrinsic dynamic performances of PV power, pumped water, induced drawdown. In this work, the optimization is based on hourly dynamic models of the crop water requirements, pumped water and groundwater response to pumping and crop yield. The optimization process is led using hourly data for the crop irrigation season occurring from the beginning of April to the end of July [21].

3 Modelling the PVWP system

The dynamic simulation of a PVWP system needs the models of photovoltaic array, inverter and water pump, crop water demand, groundwater response to pumping and crop growth as shown in Figure 2. The PV array model calculates the conversion of solar radiation into power. The inverter–pump model simulates the behaviour of the power conditioning system and pump according to the power generated by the PV array. The crop water demand model is used to assess the crop water requirements both for designing and simulation purposes. The groundwater supply and crop growth models simulate the effect of water pumping on the groundwater level and crop yield, respectively. To ensure a correct and continuous operation of the system and for a sustainable exploitation of the groundwater, the groundwater resources have to be more abundant than the water demand. The description of the hydraulic head model has been omitted in this work since it relies on the common laws of hydraulic. Alfalfa (*Medicago Sativa*) is used as reference crop in this paper since it is the growing crop at the PVWP pilot site tested in this paper.

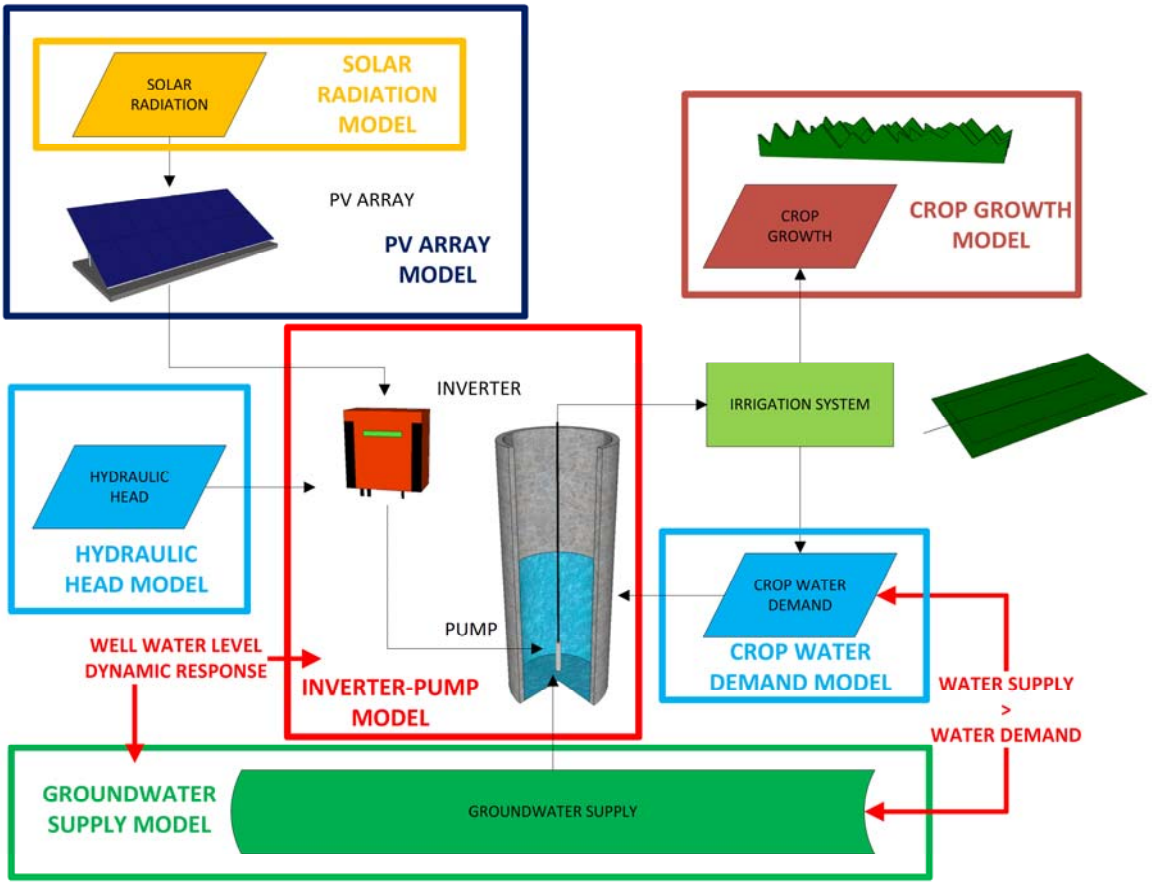

Figure 2: Overview of the modelling blocks of an integrated PVWP system.

3.1 Photovoltaic array

Photovoltaic (PV) modules convert the total solar radiation received onto the tilted surface into electricity. The total solar radiation $G_{g,t}$ (W) depends on the horizontal radiation, surface orientation and it is given by three different contributions: beam radiation $G_{b,t}$ (W), diffuse radiation $G_{d,t}$ (W) and reflected radiation $G_{r,t}$ (W):

$$G_{g,t} = G_{b,t} + G_{d,t} + G_{r,t} \quad (5)$$

The beam component of the global tilted radiation can be calculated from the horizontal radiation through the following equation presented in Duffie et al. [34]:

$$G_{b,t} = \frac{G_{g,h} - G_{d,h}}{\cos(90 - \alpha)} \cos(\theta) \quad (6)$$

Where, $G_{g,h}$ is the global horizontal radiation (W), $G_{d,h}$ is the diffuse horizontal radiation (W), α is the solar altitude (˚) and θ is the angle of incidence (˚). The angle of incidence θ, function of the declination angle δ (˚), latitude φ (˚), tilt angle β (˚), azimuth angle γ (˚) and hour angle ω, has been computed according to the procedure described in Duffie and Beckman [34]. The diffuse component is given by:

$$G_{d,t} = G_{d,h} \frac{1 + \cos(\beta)}{2} \quad (7)$$

The ground reflected radiation is given by the following relation:

$$G_{r,t} = \rho_g G_{d,h} \frac{1 - \cos(\beta)}{2} \quad (8)$$

Where, ρ_g is the ground reflectance. The hourly values of the global horizontal radiation and of the diffuse horizontal radiation have been taken as input for the solar radiation model. The required hourly data of solar radiation were collected from the weather station located nearby the tested PVWP system. According to Duffie and Beckman [34], the hourly power output from the PV array P_{PV} (W) is given by:

$$P_{PV} = \eta_{PV} A_{PV} G_{g,t} \quad (9)$$

Where, η_{PV} is the efficiency of the PV module (%) and A_{PV} is the PV array area that depends on the PV power peak capacity installed. η_{PV} is given by the following equation [34]:

$$\eta_{PV} = \eta_{PV,STC} \left[1 + \frac{\mu}{\eta_{PV,STC}} (T_a - T_{STC}) + \frac{\mu}{\eta_{PV,STC}} \frac{(NOCT - 20)}{800} (1 - \eta_{PV,STC}) G_{g,t} \right] \quad (10)$$

Where, $\eta_{PV,STC}$ is the efficiency of the PV module at standard test conditions (STC), μ is the temperature coefficient of the output power (%/°C), T_a is the ambient temperature (°C), T_{STC} is the standard test conditions temperature (25°C) and *NOCT* is the nominal operating cell temperature (°C). According to Duffie and Beckman [34], the temperature coefficient of the output power μ can be approximated to:

$$\mu \approx \eta_{PV,STC} \frac{\mu_{V_{oc}}}{V_{mp}} \tag{11}$$

Where, μ_{Voc} (V/°C) is the open circuit voltage temperature coefficient and V_{mp} (V) is the voltage at maximum power point. Table 2 summarizes all the characteristic parameters of the PV modules simulated in this paper.

263 Table 2: Characterizing parameters of the PV module (CEEG SST 160-72P) [35].

I_{mp} (A)	4.6
V_{mp} (V)	34.8
I_{sc} (A)	5.16
V_{oc} (V)	43.8
Area (m²)	1.32
$\eta_{PV,STC}$ (%)	12.56
μ_{Voc} (V/°C)	-0.147
NOCT (°C)	45

264 **3.2 Inverter-water pumping system**

265 The water pumped by a PVWP system significantly depends on the dynamic variability of the
266 solar radiation, ambient temperature, performances of the inverter and the pumping system.
267 Solar radiation and ambient temperature affect primarily the power output from the PV array
268 whereas the ambient temperature and the supplied power affect the efficiencies of the
269 inverter and pump. The efficiency of the inverter has been taken from an inverter database
270 and set to 95% [36]. The pump efficiency curve (water flow versus power input for a given
271 head) has been calculated from the standard characteristic pump curve (head versus water
272 flow) according to the following set of equations derived from the affinity laws and compiled
273 by Abella et al. [37]:

274 $$Q_o = Q_r \sqrt{\frac{H_o}{H_r}} \quad (12)$$

$$P_{p,o} = \rho g H_o \frac{Q_r}{\eta_p} \sqrt{\frac{H_o}{H_r}} \quad (13)$$

$$P_{PV} = \frac{P_{p,o}}{\eta_{m,o} \eta_{inv}} \quad (14)$$

Where, Q_o (m^3/h) is the operational water flow corresponding to the operational hydraulic head H_o (m), Q_r is the reference water flow (m^3/h) at the reference hydraulic head H_r (m) from the pump standard characteristic curve, $P_{p,o}$ is the operational pump power (W), $\eta_{m,o}$ is the efficiency of the motor at the corresponding working conditions and η_{inv} is the efficiency of the inverter (%).

3.3 Irrigation water requirements

The assessment of the water demand plays a key role in the design of the PV array, pumping unit and irrigation system. Moreover, the evaluation of the crop water requirements is significant in order to guarantee a sustainable and efficient management of the water resources, since the water demand cannot exceed the available water resources. The water demand for the entire crop cycle is strictly bounded to the climatic conditions of the specific site, especially air humidity, ambient temperature, solar radiation, wind speed and precipitation. The crop water demand and yield response to water is typically determined from the reference evapotranspiration ET_0. The daily and hourly assessment of the crop water demand has been evaluated using the FAO Penman-Monteith method [38]. The hourly reference evapotranspiration ET_0 (mm/hour) is given by the following relationship:

$$ET_0 = \frac{0.408\,\Delta\,(R_n - G) + \gamma \frac{37}{T_a + 273}\,u_2\,(e_s - e_a)}{\Delta + \gamma\,(1 + 0.34\,u_2)} \quad (15)$$

Where, R_n is the net radiation at the grass surface (MJ/m^2 hour), G is the soil heat flux density (MJ/m^2 hour), T_a is the mean hourly air temperature (°C), Δ is the saturation slope of vapor pressure curve at T_a (kPa/ °C), γ is the psychrometric constant expressed (kPa/°C), e_s is saturation vapour pressure (kPa), e_a is the average hourly actual vapour pressure (kPa) and u_2 is the average hourly wind speed (m/s). The irrigation water requirements have been assessed from the reference evapotranspiration ET_0, calculating the evapotranspiration in cultural conditions ET_c, the effective precipitation P_e and taking into account the efficiency of the irrigation system. The procedure to compute the irrigation water requirements is thoroughly described in Campana et al. [15] and in Allen et al. [38].

3.4 Crop growth model

To evaluate the benefits of PVWP systems, predicting the crop yield corresponding to the water supply represents a key issue. In 1970s, FAO proposed a relationship between crop yield and water supply to predict the reduction in crop yield. The crop-water production function relates the relative yield reduction to the relative reduction in evapotranspiration and is given by Allen et al. [38]:

$$\left(1-\frac{Y_a}{Y_m}\right)=K_y\left(1-\frac{ET_a}{ET_c}\right) \quad (16)$$

Where, Y_a is the actual yield (tonne DM/ha), Y_m is the maximum yield (tonne DM/ha), K_y is the yield response factor, ET_a is the actual evapotranspiration (mm/hour) and ET_c is the evapotranspiration in cultural conditions with no water stress (mm/hour). The actual yield Y_a represents the crop yield reduction compared to the maximum due to a reduction in the water provided through irrigation. The maximum Alfalfa yield Y_m used in the simulations has been assumed equal to 8 tonne DM/ha year as confirmed by a local specialist of the studied area

316 [39]. The yield response factor K_y simplifies the complex natural procedures that rule the effect
317 of water deficit on the crop productivity. K_y for Alfalfa is equal to 1.1 as given by Allen et al.
318 [38]. The actual evapotranspiration ET_a depends on the available water supply to the crop
319 (both through irrigation and rainfall) and on the soil parameters. The soil parameters assumed
320 in this work were taken from a previous work conducted in the same studied area [21]. The
321 procedure adopted to calculate the actual evapotranspiration ET_a is thoroughly described in
322 Allen et al. [38]. Several papers have used the crop-water production function for estimating
323 the crop productivity: Garg and Dadhich [40] used and validated the crop yield function for
324 assessing the effect of deficit irrigation on eight different crops in India; Igbadun et al. [41]
325 compared four different crop-water production functions for evaluating the effect of deficit
326 irrigation on maize. It resulted that Equation 16 was the best for simulating the crop yield. In
327 this paper, the crop-water production function has been used as direct method to simulate
328 the crop yield on the basis of the water supplied by the PVWP system. The crop yield
329 simulations together with the crop prices have been used to evaluate the revenues generated
330 by the PVWP system operation in order to identify the optimal point between revenues, costs
331 and constraints.

332 **3.5 Groundwater supply model**

333 The modelling of the aquifer response to the PVWP system operation is of significant
334 importance for predicting the drawdown *s* (the lowering of the water level in the well
335 compared to the static water level) and then the effective dynamic head of the pumping
336 system. During the operation of PVWP system, the drawdown *s* results in unsteady conditions
337 for most of the time due to the dynamic variation of the power output from the PV array.
338 Typically, groundwater transient modelling is based on Theis equation, which gives the

unsteady distribution of the drawdown *s* at a radial distance *r* and at the time *t* under the following assumptions: (I) homogeneous and isotropic confined aquifer, (II) no source recharging the aquifer, (III) aquifer compressible, (VI) water released instantaneously as the head is lowered and (V) constant pumping flow [42]. The assumption regarding the constant pumping is unrealistic for PVWP system application and make the Theis equation inappropriate for groundwater flow modelling. The analytical solutions of the equations governing groundwater flows assuming inconstant pumping flows were obtained by Ospina et al. [43]. In this work, the method proposed by Rasmussen et al. [44] is used to simulate the drawdown. If the pumped water and the characteristic of the aquifer are known, the following equation calculates the drawdown *s*:

$$s(r,t) = \frac{Q_0}{2\pi T} K_0\left(r\sqrt{\frac{i\omega}{D}}\right) \quad (17)$$

Where, *r* is the distance from the pumping well assumed equal to 1 m, *t* is the time variable (1h), Q_0 is the pumping rate (m^3/h), *T* is the aquifer transmissivity (m^2/h), K_0 is the zero-order modified Bessel function, *i* is the imaginary number, ω is the pumping frequency (given by the ratio between 2π and *p*, the pumping cycle) (Hz) and *D* is the hydraulic diffusivity (m^2/h). The aquifer transmissivity and the hydraulic diffusivity were taken from the pumping tests carried out by Zhang et al. [45].

3.6 Model validation

To obtain the optimal results, it is of great importance to select the models that can simulate the PVWP system accurately and provide correct inputs to the optimization. In the work conducted by Glasnovic and Margeta [12], the models were not carefully validated. In this

work, measurements have been conducted at a pilot PVWP system and the models used in optimization have been validated against the measurements.

3.6.1 Measurements at the pilot PVWP system

The tested PVWP system is located in the Wulanchabu desert grassland area, Inner Mongolia, China, which latitude, longitude and altitude of the site are 41.32˚ N, 111.22˚ E and 1590 m above the mean sea level. It is used to provide water for 1 ha of Alfalfa cultivated field. The main system components and PV array orientation angles are listed in Table 3.

Table 3: PVWP system components and characteristics.

Number PV modules	9
PV power (kW_p)	1.44
Pump (kW)	1.1 (AC centrifugal)
Tilt angle (°)	42
Azimuth (°)	-36

To avoid dry running of the motor-pump, a water level probe is installed on the upper part of the pump. If the water level in the well reaches the probe, the inverter shuts down and makes attempt to restart each 30 minutes. The well is marked out by a static water level of 5 m below the ground surface. The pump is positioned at the bottom of the well, at 3.5 m depth from the static water level. The pump safety probe is installed on the top of the pump, at 2.5 m depth from the static water level. To measure the variation of the well water level, a water pressure probe with data logger is installed at the bottom of the well. The PVWP system has been tested in two different scenarios: recirculation scenario (S1) - the water lifted up by the pumping system was recirculated back into the well; and micro irrigation scenario (S2) - the

water lifted up from the well is pumped directly into a micro irrigation system located about 150 m far from the well. S1 has aimed to test the pumping system and to validate the models regarding the PVWP system. The main purpose of S2 was to analyse the effects of pumping on the groundwater level. To measure the water pumped from the well, two flow meters are installed along the pipeline network. All the performed measurements and the corresponding used instruments are listed in Table 4. Figure 3 shows a schematic diagram of the tested PVWP system scenarios together with the instruments used for gathering the operational data.

Table 4: Measurement carried out during the tests and the corresponding instruments and resolutions.

Measurements	Instrument	Logging time	Resolution
Solar radiation	Pyranometer	1 hour	± 1 W/m^2
Power	DC/AC power meter	1 hour	± 1 W
Water flow	Flowmeter	1 hour	± 0.001 m^3
Well water table	Pressure sensor	1 hour	± 0.02 mwc
Evapotranspiration	Weighing lysimeter	1hour	± 0.02 mm

The measured data about solar radiation, power output and water flow were used to validate the PVWP system model, in particular the pump efficiency curve (water flow versus power input for a given head). The measurements of the well water level were used to validate the model related to the groundwater level response to pumping. The weighing lysimeter data

393 were compared with the modelled data of evapotranspiration to validate the model used to
394 calculate the crop water demand.

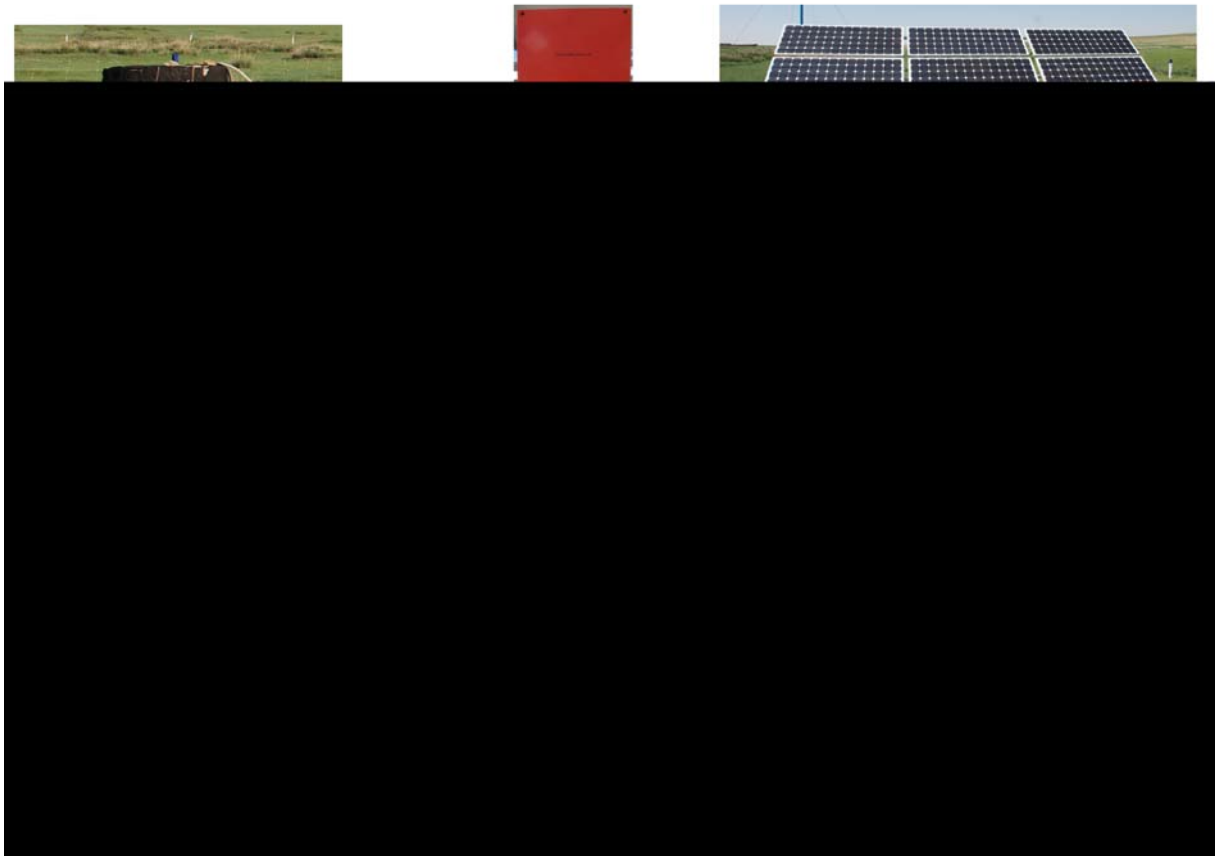

395

396 Figure 3: Schematic diagram of the system configurations used during the tests.

397

398 It has to be pointed out that the tests carried out in irrigation scenario (S2) aimed to analyse
399 the effects of PVWP system operation on the groundwater level and to introduce the novel
400 optimization procedure for PVWP systems for irrigation.

401 **3.6.2 PVWP models validation**

402 Figure 4 compares the simulated results and the measured water flow. Good agreement is
403 observed at power inputs lower than 800 W. The discrepancy between modelled data and
404 measured data is higher at higher PV power inputs due to the system configuration: PVWP

system directly connected to the irrigation system. At high power inputs and thus water flows, the effective operational hydraulic head can differ from the fixed hydraulic head assumed in the simulations due to pressure variation in the irrigation system. The water flow for power input lower than 250 W becomes zero since the power produced by the PV system is not enough to run the pumping unit.

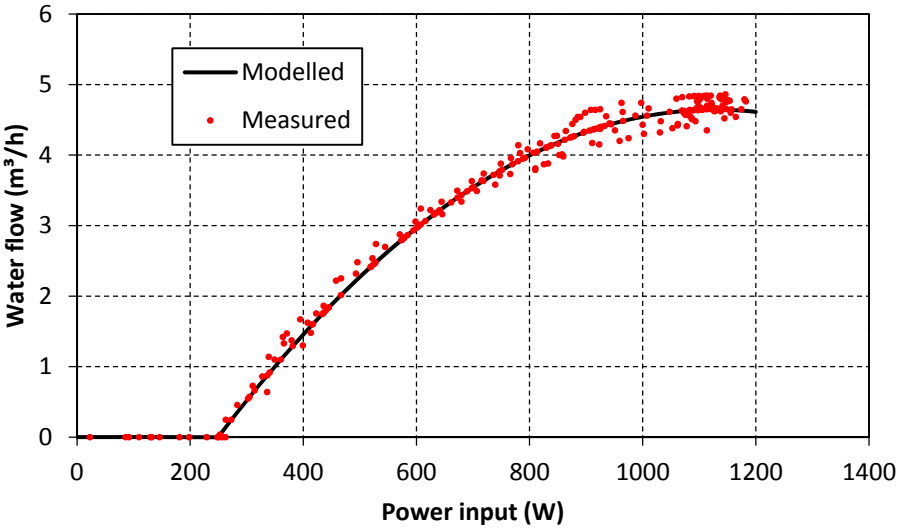

Figure 4: Pumping tests in recirculation scenario.

Figure 5 compares the simulated results and the measured data about the reference evapotranspiration. The measured data have been reconciled by the outliers produced during the precipitation events. In general, the calculated results agree well with the measured data. The discrepancies between measured and calculated data are caused by the pressure of wind gusts on the lysimeter, objects on the lysimeter and temperature effects.

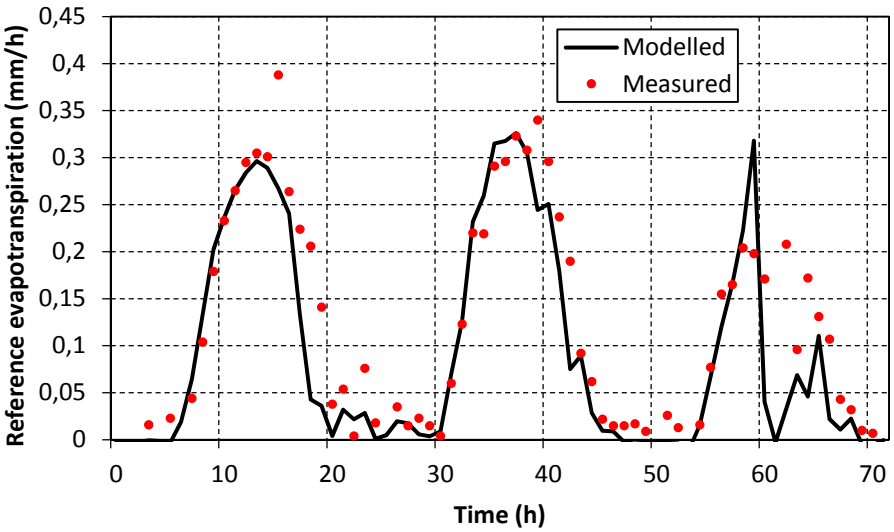

418

419 Figure 5: Measured and modelled hourly evapotranspiration data.

420 Figure 6 shows the modelled results and field measurements of the drawdown as a function

421 of the water flow.

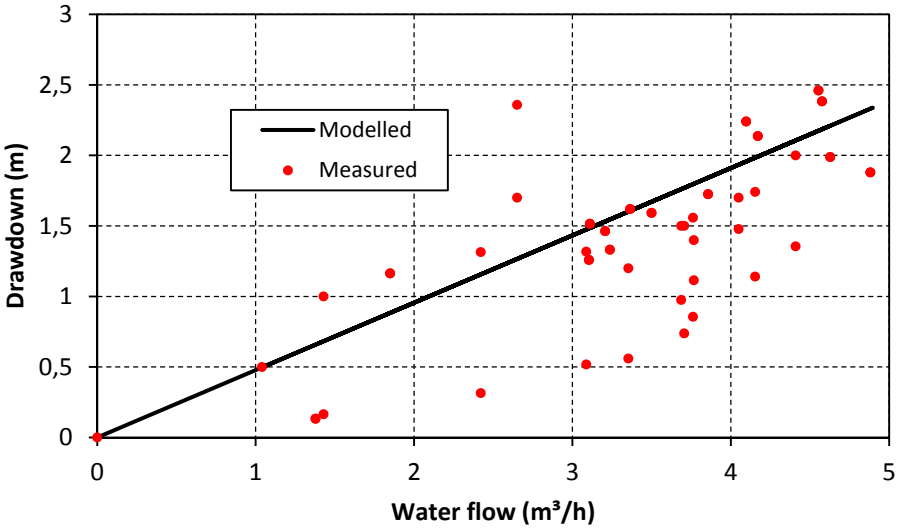

422

423 Figure 6: Measured and modelled hourly groundwater level.

424 The discrepancy may be caused by the poor borehole construction technique, inadequate and

425 low accuracy instrumentation and field conditions. Nevertheless, it has to be pointed out that

426 the maximum deviation between measured and modelled data at the highest pumping rate is
427 less than 0.5 m. It implies that the model can be considered suitable to describe at least the
428 maximum pumping effect in terms of drawdown. Moreover, it has to be emphasized that the
429 same model showed an excellent agreement with the field measurement data in previous
430 tests carried out by Rasmussen et al. [44] at different aquifers with high accuracy equipment.

431 # 4 Optimization results and discussions

432 ## 4.1 Identified problem

433 Figure 7 shows the measured pumped water as a function of the solar radiation and the water
434 level in the well. Since the pumped water by the PVWP system is larger than the recharge rate
435 of the well, the groundwater table declines. Therefore, it implies that the designed PVWP
436 system was oversized. To avoid dry-up conditions, the inverter safety control system stops the
437 pump and the operation of the system is interrupted after 12 pm every half hour. Although
438 there is still abundant solar radiation and thus power from the PV array, the pumped water
439 volume decreases of about half. To overcome the encountered problem, it would have been
440 significant to test the recharge rate of well before the installation of the PVWP system.
441 Moreover, it has to be pointed out that the water availability in the well can notably vary from
442 year to year, especially from wet to dry year, affecting consequently the system design and
443 the irrigable area.

444

445

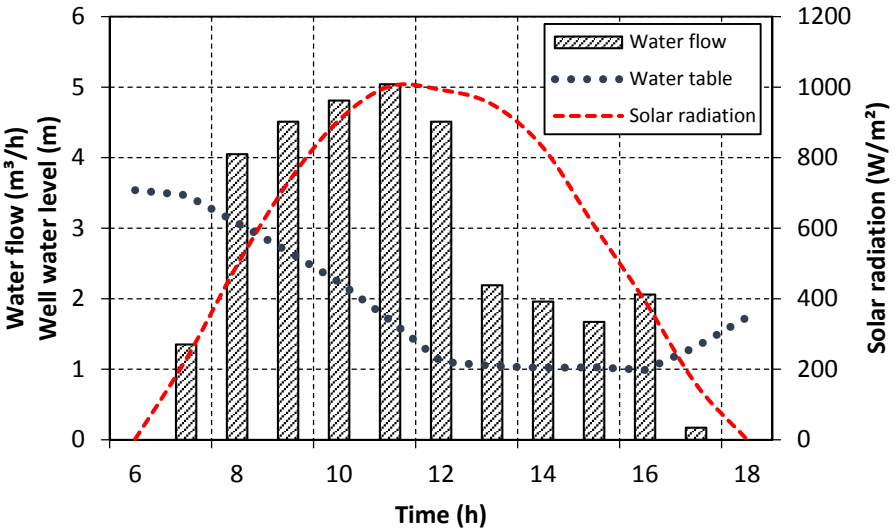

446

447 Figure 7: Pumping tests in irrigation scenario as function of the solar radiation and water

448 level in the well.

449 Another issue related to the operation of the studied PVWP system is the discrepancy

450 between crop water requirements and pumped water. The calculated monthly Alfalfa water

451 requirement varies a lot during the irrigation season registering its peak in June, as shown in

452 Fig 8. Comparing the modelled pumped water with the water demand, it is clear that the

453 PVWP system is unable to meet the irrigation water requirement for most of the irrigation

454 season.

455

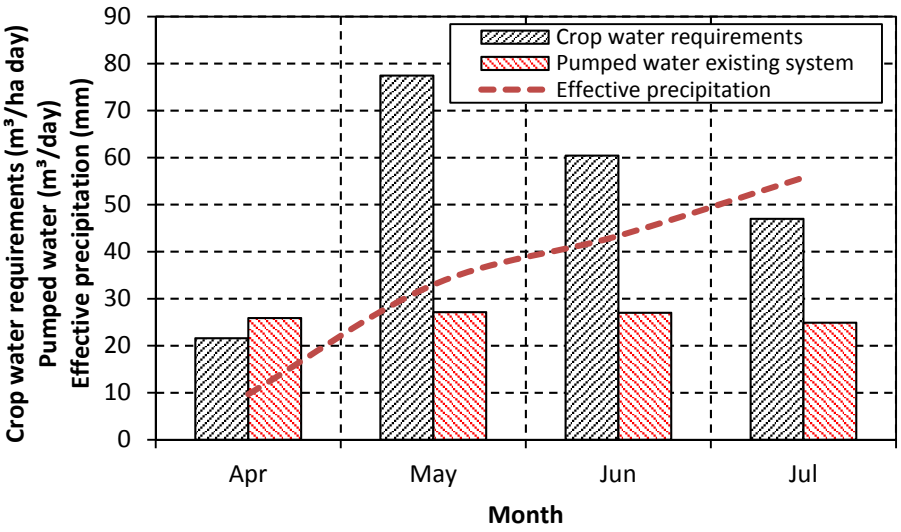

456

457 Figure 8: Alfalfa water demand, effective rainfall and pumped water from the existing PVWP

458 system.

459 On one hand the PVWP system is oversized since the water level in the well reach the bottom;

460 but on the other hand the PVWP system is also undersized since it cannot supply the crop

461 water need during the irrigation season. It has to be pointed out that the procedure adopted

462 to design the existing PVWP system is unknown and not led by the authors of this paper.

463 **4.2 System optimization**

464 Using the approach given in section 2.6, the existing system has been optimized assuming a

465 maximum hourly drawdown s_h equal to 2.5 m that corresponds to the depth of the pump h_p

466 measured from the static water level. Table 5 summarizes the characteristic parameters

467 (decision variables, operation failures, *ICC*, Alfalfa yield and *PBP*) for the existing and optimized

468 PVWP system.

469

470

Table 5: Existing and optimized PVWP characteristic parameters.

Parameter	Existing system	Optimized system
Number PV modules	9	6
PVWP capacity (kW_p)	1.44	0.96
Pump capacity (kW)	1.1	1.1
Tilt angle (°)	42	10
Azimuth (°)	-36	8
ICC (US$)	4800	3900
Failures (time)	350	0
Y_a (tonne DM/ha)	2.7	2.6
PBP (years)	> lifetime (forage price 207 $/tonne DM)	16 (forage price 207 $/tonne DM)

The constraint due to the decline of the groundwater level reduces the PVWP capacity. As a result, the PV size is decreased from 1.44 kW_p to 0.96 kW_p. In addition, the optimization of the tilt and azimuth angle allows an increase of 10% in the PV power output during the irrigation season compared to the existing orientation. The optimal tilt angle maximize the solar irradiation harvested by the PV array during the irrigation period between April and July. Figure 9 shows the effect of tilt angle on the annual revenues R_{ann}.

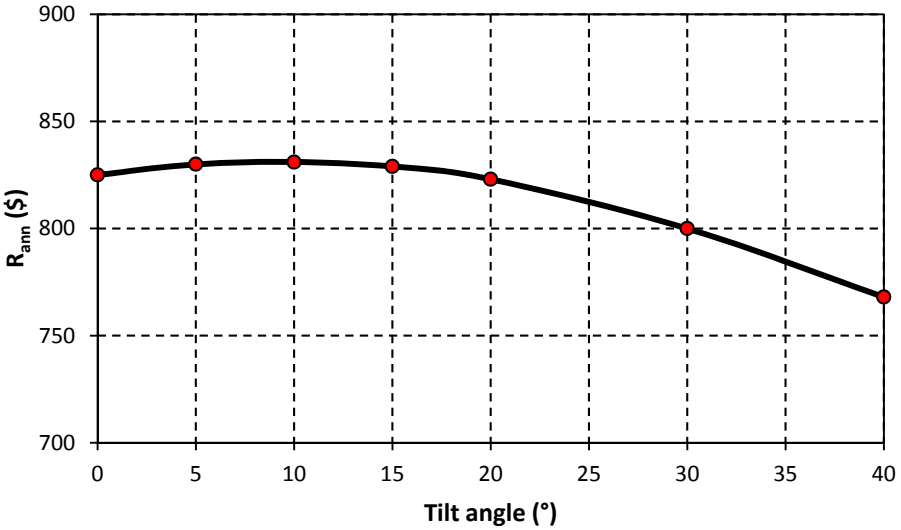

479

480 Figure 9: Effect of tilt angle on the annual revenues.

481 The optimal tilt angle causes an increase of the annual revenues of about 8% compared to the
482 tilt angle of the existing system. The *ICC* for the existing system is 4800 US$. The main cost
483 item is represented by the PV modules accounting for 60% of the *ICC*, followed by engineering
484 and installation costs and inverter representing a share of 17% and 14%, respectively. The *ICC*
485 for the optimized system is 3900 US$, corresponding to a reduction in the *ICC* of 18.8%
486 compared to the current PVWP system. The reduction in investment cost is mainly due to the
487 less investment in PV modules and inverter and the resulting reduction in project
488 implementation costs.

489 In addition, the continuous operation is guaranteed during the whole irrigation season.
490 Compared to the 350 times that the existing system is shut down to avoid dry-up, the
491 optimized system never reaches the set level corresponding to the safety probe. Figure 10
492 shows the well water level trend for the optimized system during the irrigation season.

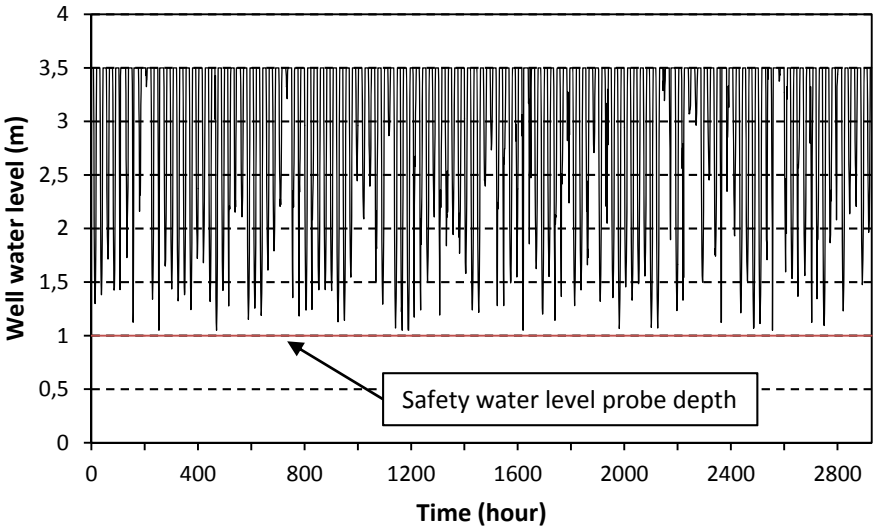

493

494 Figure 10: Well water level trend induced by the optimized system during the irrigation

495 season.

496 To clearly illustrate the operation difference between the existing system and the optimal

497 system, dynamic simulations were conducted with a time step of 10 minutes for two days in

498 June. Figure 11 and 12 show the results of water flow and well water level. The optimal system

499 operates between 8 am and 6 pm reaching an hourly maximum flow rate of about 3.9 m^3/h

500 (0.65 m^3/10 min) around 12pm, producing a maximum drawdown of 2.3 m (equivalent to a

501 minimum well water level of 1.2 m) without reaching the water level probe (installed at 1

502 meter depth). On the contrary, the existing system is shut down in every hour after 12pm.

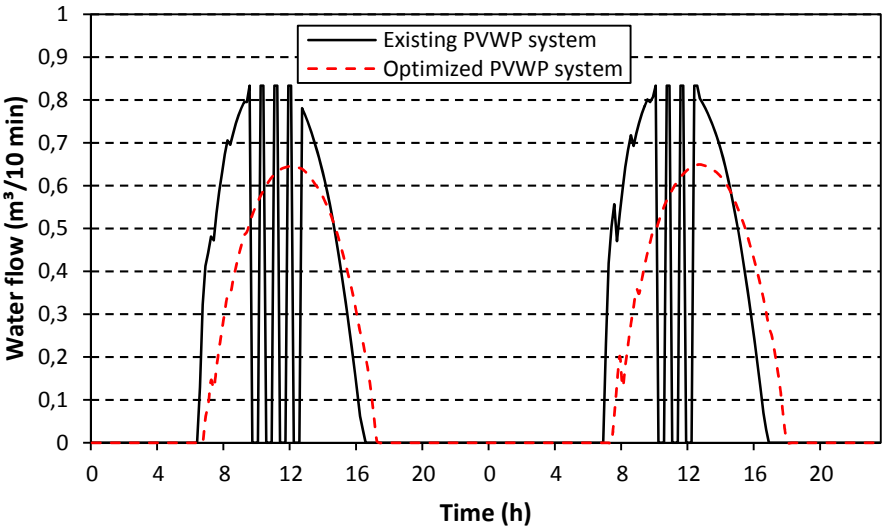

503

504 Figure 11: Simulations of the pumped water and well water level for the existing and

505 optimized PVWP systems.

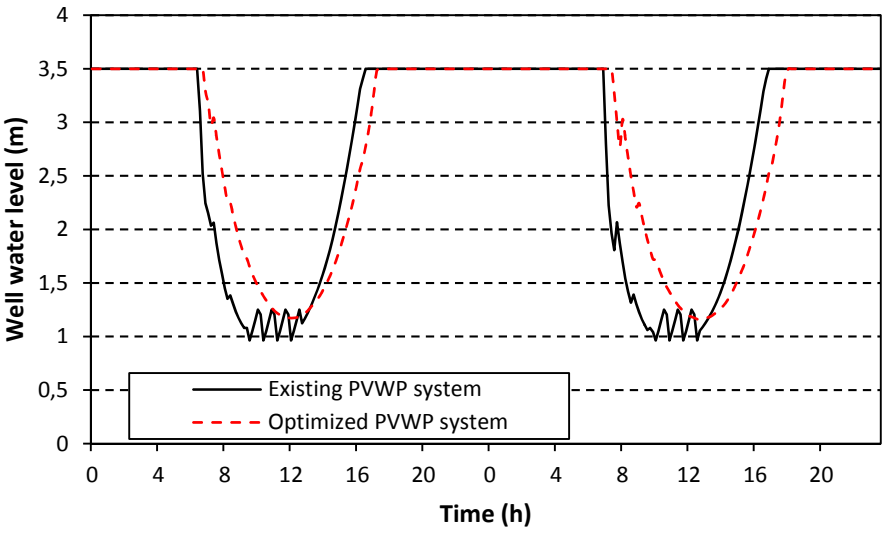

506

507 Figure 12: Simulations of the well water level for the existing and optimized PVWP systems.

508 Despite the decreased PV size, the effects of the pumped water on the crop yield in

509 insignificant due to the continuous shutdowns of the current installed PVWP system. The

510 resulting annual crop yields at the end of the irrigation season are 2.7 and 2.6 tonne DM/ha

511 for the existing system and the optimized system, respectively. Since the save from the *ICC* of
512 PV is much larger, the optimized system has a shorter *PBP* and the optimization makes the
513 PVWP system more suitable.

514 **4.3 Sensitivity study**

515 Sensitivity studies have been conducted to understand the effect of crop price and PV module
516 price, which are the key parameters for the economic analysis, on the optimization results.
517 The forage price has been set to vary between 150 and 300 $/tonne DM, whereas the PV
518 module price has been varied between 1 and 2 $/W_p$.

519 Figures 13 shows the effect of forage price on the optimal PVWP system capacity assuming a
520 constant PV module price of 1.5$/W_p$ together with the corresponding annual profit. With the
521 increase of forage price, the annual profit rises; however, the forage price doesn't affect the
522 optimal PVWP system size clearly. Similarly, there is no obvious impact on the optimal PVWP
523 system capacity from the PV modules prices either, as depicted in Figure 14. The explanation
524 is that the groundwater constraint narrows the search of the optimal PVWP system capacity
525 into a small range: between 0.25 to 0.96 kW_p (the lower threshold corresponds to the
526 minimum power peak to run the pumping system whereas the upper threshold corresponds
527 to the maximum power peak to avoid an excessive drawdown). The search of the optimal
528 PVWP system capacity is thus limited in a region where both the crop yield, and thus the
529 annual revenues, and the PVWP system cost functions have a linear trend. Accordingly, the
530 effects of PV module and forage price variation have a negligible effect in the search of the
531 optimal system size.

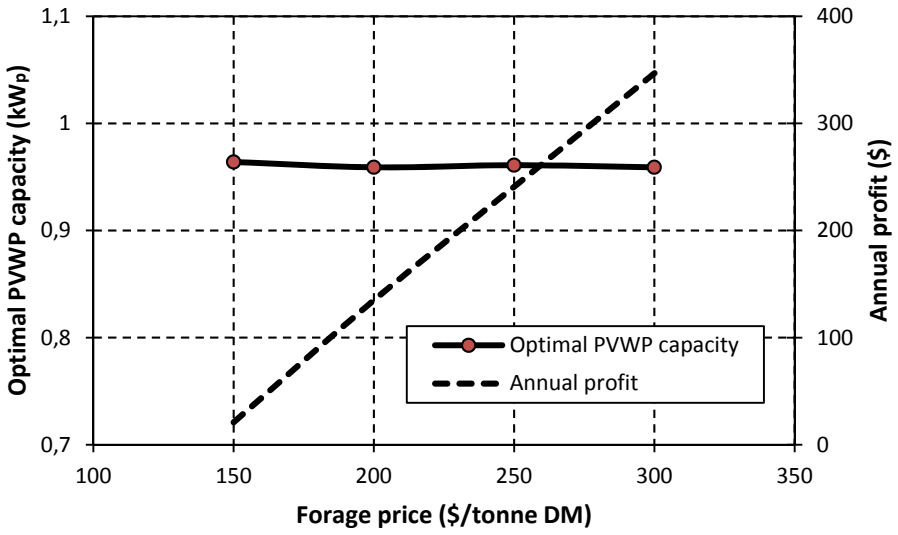

532

533 Figure 13: Effect of forage price on the optimal PVWP system size and annual revenues

534 assuming a constant PV module price of 1.5$/$W_p$.

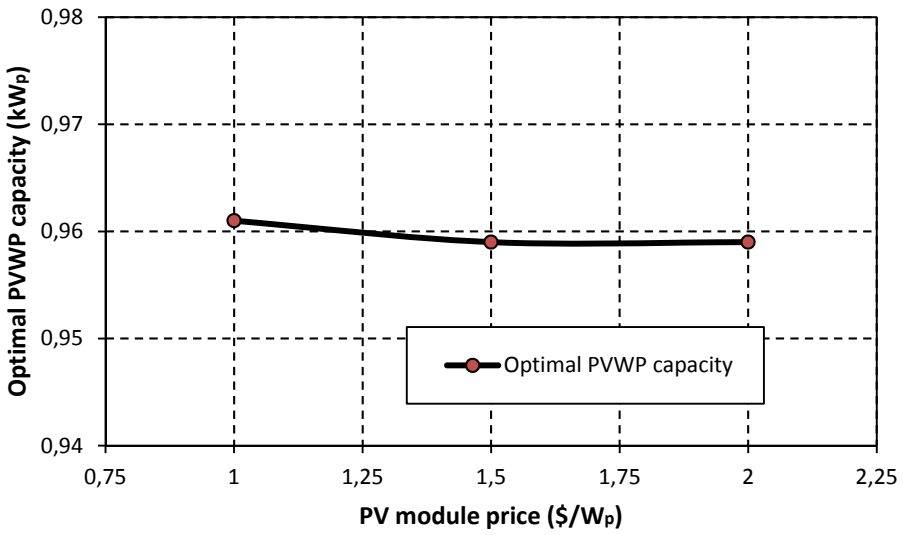

535

536 Figure 14: Effect of PV module price on the optimal PVWP system capacity assuming a

537 constant forage price of 200 $/tonne DM.

538 As an example, Figure 15 shows the effect of the groundwater level constraint and PV module

539 price on the maximization of the annual profit, assuming a constant forage price of

150$/tonne DM. If the ground water constraint is taken into account, the optimal PVWP system capacity that maximizes the annual profit is 0.96 kW_p, independently from the PV module price. Nevertheless, if the groundwater level constraint is disregarded, since the relationship between PVWP system capacity and crop yield is nonlinear, the price of PV modules has more obvious impacts on the optimal PVWP system capacity that maximizes the annual profit (2 and 2.2 kW_p for PV module price of 2.0 and 1.0 $\$/W_p$, respectively).

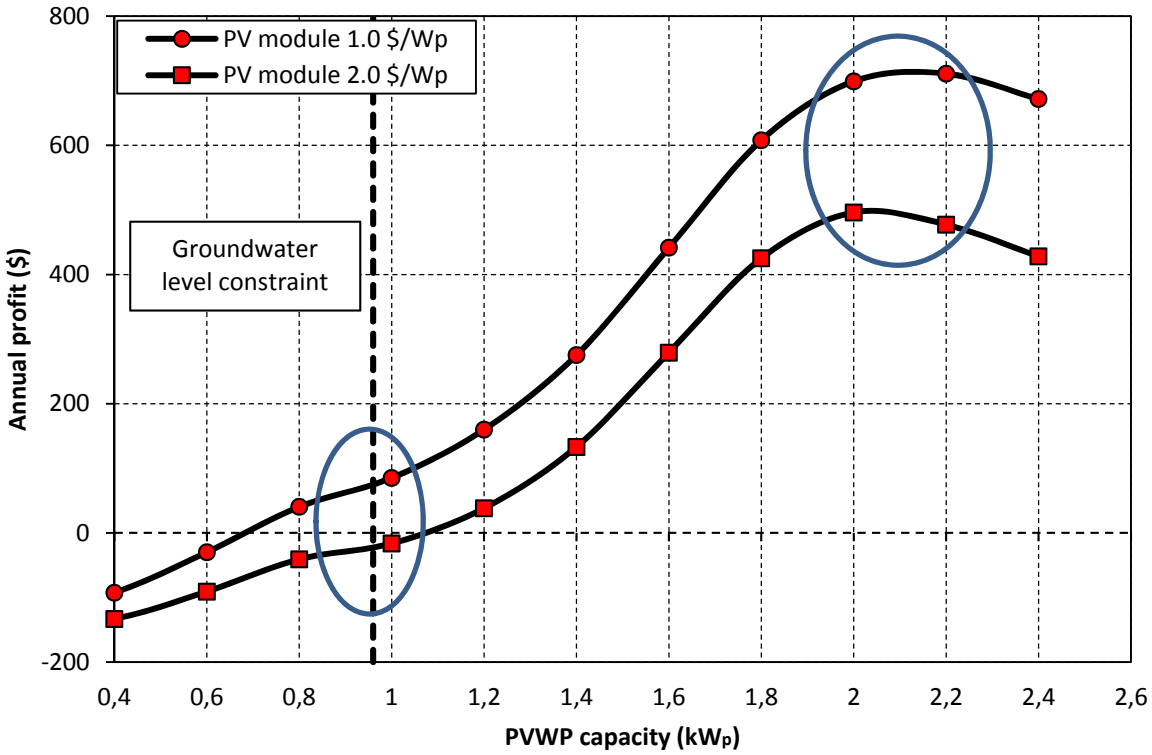

Figure 15: Effect of the groundwater level constraint on the optimal PVWP system capacity.

To identify those effects, the same sensitivity analyses have been conducted without the constraint of the groundwater level. Results are shown in Figure 16. The variation of PV modules and forage prices result in opposite trends. The increase of the forage price intends

552 to raise the PVWP capacity; while the increase of PV price intends to reduce the capacity. The
553 effect of the sensitive parameters variation on the PVWP system capacity is about 10%. The
554 results show the effectiveness and importance of considering the economic aspects into the
555 optimization of PVWP systems for irrigation, especially for large applications where the
556 optimization design can lead to significant economic benefits.

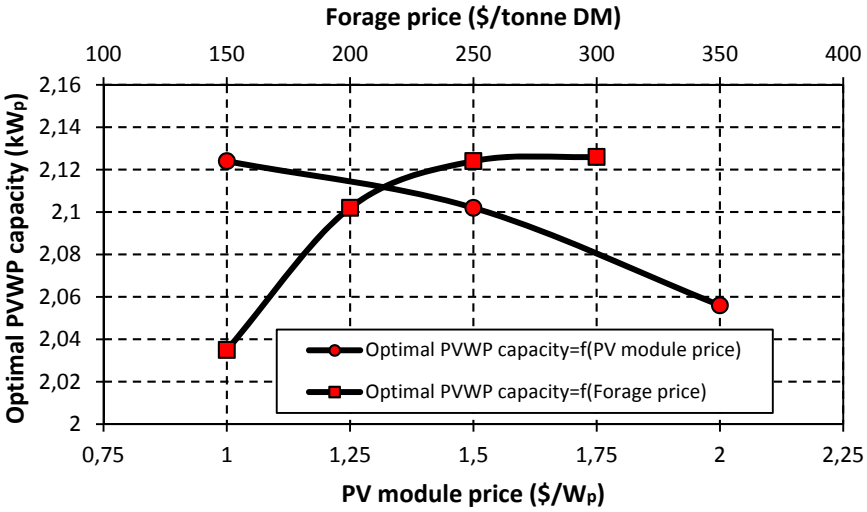

557

558 Figure 16: Effect of forage price and PV module price on the optimal PVWP system size
559 assuming no groundwater response constraint.

560 The groundwater level constraint has played the key role in determining the optimal size of the PVWP
561 system, assuming no system failures during the irrigation season (maximum reliability of the PVWP
562 system in terms of operation continuity). The PV modules and forage price can affect the optimal PVWP
563 system size but only if the drawdown is not a limiting factor. The optimization and simulation results
564 show also how the groundwater level constraint is significant for ensuring high crop productivity and
565 thus high PVWP system profitability.

5 Conclusions

A new approach to optimize the photovoltaic water pumping (PVWP) system for irrigation has been proposed with the consideration of groundwater response and economic factors in this paper. Applying the proposed approach to an existing system shows a reduction in PV module size (from 1.44 down to 0.96 kW_p). This implies a decrease of 18.8% in the investment capital cost and therefore improve the economic feasibility of PVWP clearly. Even though the prices of crop and PV modules are the key parameters concerning the economic feasibility, according to the sensitivity study, they don't have clearly effects on the optimal system capacity if the ground water level is limited. However, if the groundwater level response to pumping does not represent a constraint, the increase of the forage price intends to raise the PVWP capacity; while the increase of PV price intend to reduce it.

Acknowledgments

The authors are grateful to the Swedish International Development Cooperation Agency (SIDA) and Swedish Agency for Economic and Regional Growth (Tillväxtverket) for the financial support.

References

[1] Longjun C., "UN Convention to combat desertification", Encyclopedia of Environmental Health, 2011, DOI: http://dx.doi.org/10.1016/B978-0-444-52272-6.00654-1.

[2] Yan J., Gao Z. Wang H. Liu J., "Qinghai pasture conservation using solar photovoltaic (PV)-driven irrigation", Asian Development Bank, Project Report, 2010.

586 [3] Bouzidi B., Haddadi M., Belmokhtar O., “Assessment of a photovoltaic pumping system in
587 the areas of the Algerian Sahara”, Renewable and Sustainable Energy Reviews 13 (2009) 879–
588 886.
589 [4] Hrayshat E.S., Al-Soud M.S., “Potential of solar energy development for water pumping in
590 Jordan”, Renewable Energy 29 (2004) 1393–1399.
591 [5] Bouzidi B., “Viability of solar or wind for water pumping systems in the Algerian Sahara
592 regions – case study Adrar”, Renewable and Sustainable Energy Reviews 15 (2011) 4436–
593 4442.
594 [6] Ghoneim A.A., “Design optimization of photovoltaic powered water pumping systems”,
595 Energy Conversion and Management 47 (2006) 1449–1463.
596 [7] Benghanem M., Daffallah K.O., Alamri S.N., Joraid A.A., “Effect of pumping head on solar
597 water pumping system”, Energy Conversion and Management 77 (2014) 334–339.
598 [8] Mokeddem A., Midoun A., Kadri D., Hiadsi S., Raja I.A., “Performance of a directly-coupled
599 PV water pumping system”, Energy Conversion and Management 52 (2011) 3089–3095.
600 [9] Boutelhig A., Hadjarab A., Bakelli Y., “Comparison study to select an optimum photovoltaic
601 pumping system (PVPS) configuration upon experimental performances data of two different
602 dc pumps tested at Ghardaïa site”, Energy Procedia 6 (2011) 769–776.
603 [10] Hamidat A., Benyoucef B., Hartani T., “Small-scale irrigation with photovoltaic water
604 pumping system in Sahara regions”, Renewable Energy 28 (2003) 1081–1096.
605 [11] Senol R., “An analysis of solar energy and irrigation systems in Turkey”, Energy Policy 47
606 (2012) 478–486.
607 [12] Glasnovic Z., Margeta J., “A model for optimal sizing of photovoltaic irrigation water
608 pumping systems”, Solar Energy 81 (2007) 904–916.

609 [13] Pande P.C., Singh A.K., Ansari S., Vyas S.K., Dave B.K., “Design development and testing of
610 a solar PV pump based drip system for orchards”, Renewable Energy 28 (2003) 385–396.
611 [14] Ould-Amrouche S., Rekioua D., Hamidat A., “Modelling photovoltaic water pumping
612 systems and evaluation of their CO_2 emissions mitigation potential”, Applied Energy 87 (2010)
613 3451–3459.
614 [15] Campana P.E., Li H., Yan J., “Dynamic modelling of a PV pumping system with special
615 consideration on water demand”, Applied Energy 112 (2013) 635–645.
616 [16] Amer E.H., Younes M.A., “Estimating the monthly discharge of a photovoltaic water
617 pumping system: Model verification”, Energy Conversion and Management 47 (2006) 2092–
618 2102.
619 [17] Hamidat A., Benyoucef B., “Mathematic models of photovoltaic motor-pump systems”,
620 Renewable Energy 33 (2008) 933–942.
621 [18] Luo Y., Sophocleous M., “Seasonal groundwater contribution to crop-water use assessed
622 with lysimeter observations and model simulations”, Journal of Hydrology 389 (2010) 325–
623 335.
624 [19] Campana P.E., Zhu Y., Brugiati E., Li H., Yan J., “PV water pumping for irrigation equipped
625 with a novel control system for water savings”, Proceedings of the 6th International
626 Conference on Applied Energy - ICAE2014.
627 [20] Campana P.E. Olsson A., Zhang C., Berretta S., Li H., Yan J., “On-grid photovoltaic water
628 pumping systems for agricultural purposes: comparison of the potential benefits under three
629 different incentive schemes”, Proceedings of the 13th World Renewable Energy Congress -
630 WREC XIII.

631 [21] Xu H., Liu J., Qin D., Gao X., Yan J., “Feasibility analysis of solar irrigation system for
632 pastures conservation in a demonstration area in Inner Mongolia”, Applied Energy 112 (2013)
633 697–702.
634 [22] Yu Y., Liu J., Wang H., Liu M., “Assess the potential of solar irrigation systems for sustaining
635 pasture lands in arid regions – A case study in Northwestern China”, Applied Energy 88 (2011)
636 3176–3182.
637 [23] Gao X., Liu J., Zhang J., Yan J., Bao S., Xua H., Qin T., “Feasibility evaluation of solar
638 photovoltaic pumping irrigation system based on analysis of dynamic variation of
639 groundwater table”, Applied Energy 105 (2013) 182–193.
640 [24] Gao T., Zhang R., Zhang J., “Effect of Irrigation on Vegetation Production and Biodiversity
641 on Grassland”, Procedia Engineering 00 (2011) 000–0003– 616.
642 [25] Olsson A., Campana P.E., Lind M., Yan J., “Potential for carbon sequestration and
643 mitigation of climate change by irrigation of grasslands”, Applied Energy 136 (2014) 1145–
644 1154.
645 [26] Olsson A., Lind M., Yan J., “PV water pumping for increased resilience in dry land
646 agriculture”, Proceedings of the 6th International Conference on Applied Energy - ICAE2014.
647 [27] Zhang C., Yan J., “Business model innovation on the photovoltaic water pumping systems
648 for grassland and farmland conservation in China”, Proceedings of the 6th International
649 Conference on Applied Energy - ICAE2014.
650 [28] Merei G., Berger C., Sauer D.U., “Optimization of an off-grid hybrid PV–Wind–Diesel
651 system with different battery technologies using genetic algorithm”, Solar Energy 97 (2013)
652 460–473.

653 [29] Bean R., Wilhelm J., “U.S. Alfalfa Exports to China Continue Rapid Growth”, USDA Foreign
654 Agricultural Service-Global Agricultural Information Network Report, 2011.
655 [30] The World Bank. Available at: http://data.worldbank.org/indicator/FR.INR.RINR.
656 Accessed: 1st July 2014.
657 [31] Solartech. Available at: http://www.solartech.cn. Accessed: 1st July 2014.
658 [32] Campana P.E., Olsson A., Li H., Yan J., “An economic analysis of photovoltaic water
659 pumping irrigation systems”, International Journal of Green Energy, (2015) (In press).
660 [33] SolveXL. Available at: http://www.solvexl.com/. Accessed: 1st July 2014.
661 [34] Duffie J.A., Beckman W.A., “Solar engineering of thermal processes”, 3rd ed. Wiley; 2006.
662 [35] CEEG. Available at: http://www.ceeg.cn/English/?lang=2. Accessed: 1st July 2014.
663 [36] PVsyst. Available at: http://www.pvsyst.com/en/. Accessed: 1st July 2014.
664 [37] Abella M.A., Lorenzo E., Chenlo F., “PV water pumping systems based on standard
665 frequency converters”, Prog. Photovolt: Res. Appl. 2003; 11:179–191 (DOI: 10.1002/pip.475).
666 [38] Allen R.G., Pereira L.S., Raes D., Smith M., “Crop evapotranspiration. Guidelines for
667 computing crop water requirements”, FAO, 1998.
668 [39] Zhang, R. 2013. Personal communication. Institute of Water Resources for Pastoral Areas,
669 Hohhot, China.
670 [40] Garg N.K., Dadhich S.M., “A proposed method to determine yield response factors of
671 different crops under deficit irrigation using inverse formulation approach”, Agricultural
672 Water Management 137 (2014) 68–74.
673 [41] Igbadun H.E., Tarimo A.K.P.R., Salim B.A., Mahoo H.F., “Evaluation of selected crop water
674 production functions for an irrigated maize crop”, Agricultural water management 94 (2007)
675 1–10.

676 [42] Kruseman G.P., “Analysis and evaluation of pumping test data”, 2nd ed., ILRI, 1994.
677 [43] Ospina J., Guarin N., Velez M., “Analytical solutions for confined aquifers with non-
678 constant pumping using computer algebra”, Proceedings of the 2006 IASME/WSEAS Int. Conf.
679 on Water Resources, Hydraulics & Hydrology, Chalkida, Greece, May 11-13, 2006 (pp7-12).
680 [44] Rasmussen T.C., Haborak K.G., Young M.H., “Estimating aquifer hydraulic properties using
681 sinusoidal pumping at the Savannah River site, South Carolina, USA”, Hydrogeology Journal
682 (2003) 11:466–482.
683 [45] Zhang J., Liu J., Campana P.E., Zhang R., Yan J., Gao X., “Model of evapotranspiration and
684 groundwater level based on photovoltaic water pumping system”, Applied Energy 136 (2014)
685 1132–1137.
686